Electronic Supplementary Material (ESI) for Materials Chemistry Frontiers.
This journal is © the Partner Organisations 2022

Supporting Information for

Memristor Based on Carbon Dots for Learning Activities of Artificial Biosynapses Applications

Xiaoyu Li[a#], Yifei Pei[a#], Ying Zhao[a], Haoqiang Song[b], Jianhui Zhao[a], Lei Yan[a], Hui He[a], Siyu Lu[b*], Xiaobing Yan[a*]

[a]Key Laboratory of brain-like neuromorphic devices and Systems of Hebei Province, College of Electron and Information Engineering, Hebei University, Baoding 071002, P. R. China.

[b]College of Chemistry and Molecular Engineering, Zhengzhou University, Zhengzhou 450000, China

*Corresponding author: Xiaobing Yan; Siyu Lu

*E-mail: yanxiaobing@ime.ac.cn; sylu2013@zzu.edu.cn

KEYWORDS: Memristor, Carbon dots, Learning method simulation, Electronic synapse

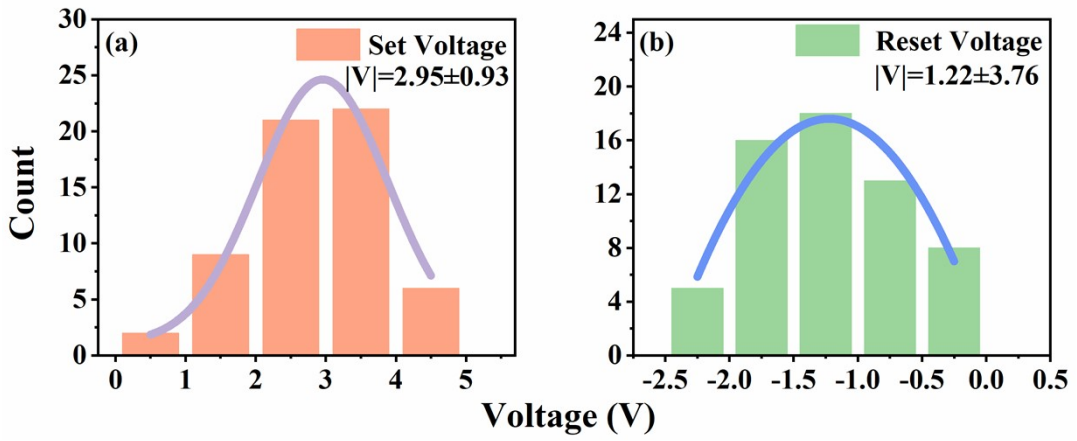

Fig. S1 SET voltages (a) RESET voltages (b) distribution for pure-HfO_2 MDs and the curves are Gaussian fits to the histograms.

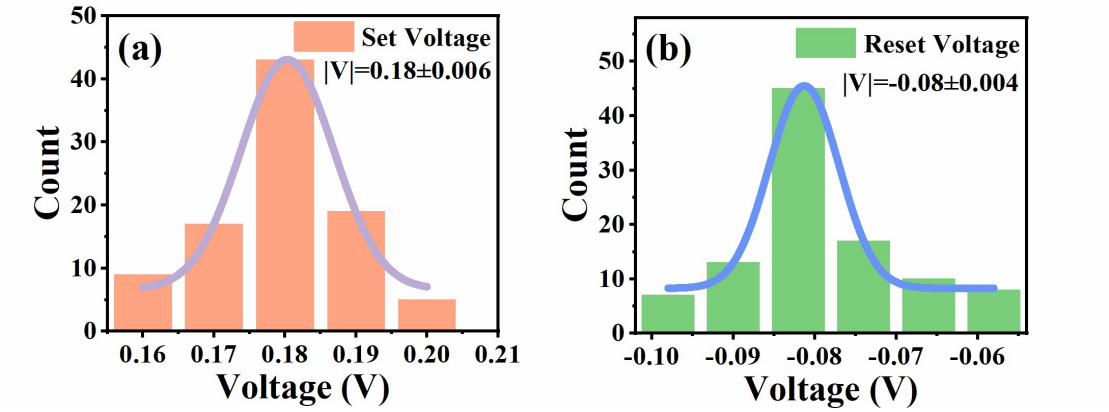

Fig. S2 SET voltages (a) RESET voltages (b) distribution for CDMDs and the curves are Gaussian fits to the histograms.

Table S1. Comparison of the performance metrics with other active electrode memristor devices.

Device structure	V_{SET} [V]	V_{RESET} [V]	R_{OFF}/R_{ON}	Retention [s]	Reference
Ag/ZrO_2/graphene/Pt	1.0 or −2.5	-1.0	-	10^4	1
Ag/SiO_x:Ag/TiOx/p^{++}-Si	2.5	-1.25	10^2	10^3	2
Ag/AgInSbTe/Ta	0.19	-0.37	-	-	3
Ag/ WS_2/Pt	3.0	-3.0	10^3	10^3	4
Ag/amorphous TiO_2/Pt	2.3	-2.3	-	-	5
Ag/S-layer protein /ITO/PET	8.0	-8.0	10^3	4×10^3	6
Ag/ZrO_2/WS_2/Pt	0.18	-0.1	10^6	4×10^4	4
Ag/graphdiyne film/ITO	1.3	-0.84	-	-	7
Ag/PVPy-Au@Ag NPs/ITO	3.0	-3.2	10^3	10^4	8
Ag/TiO_2/Al	0.68	-0.68	-	-	9
Ag/HfO_2/CDs/Pt	0.18	-0.08	10^4	2.4×10^5	This work

Table S2. Comparison of the performance metrics with other QDs memristor devices.

Device structure	V_{SET} [V]	V_{RESET} [V]	R_{OFF}/R_{ON}	Retention [s]	Reference
Ag/(InP/ZnS) QDs/ ITO	1.8	-1.5	10^2	10^4	10
Al/CdSe/ZnS QD-PMMA/ITO	2.5	-1.8	10^3	10^4	11
AgNWs/CA QDs/PVP/AgNWs/PVP	0.9	-0.9	10^6	1.1×10^4	12
Cu/PVA/MoS_2 QDs/PVA/Cu	2.3	-2.8	1.5×10^2	1.2×10^4	13
Al /MoS_2 QDs/ FTO	-2	2.4	5×10^{-4}	10^3	14
Mg/fibroin/MoS_2-QDs/ITO	1.6	-1.5	10^5	1.1×10^4	15
Ag/graphene-QDs/PVP/Ag	1.5	-1.8	10^2	-	16
ITO/$(PAH/CdSe\ QDs)_{10}$/Al	2.7	-1.5	10^2	-	17
HfO_2/Ge QDs–HfO_2/HfO_2	-	-	10^3	-	18
Ag/N-GO QDs/Ti	0.25	-	10^7	-	19
Ag/InP QDs/ITO	3.8	-2.1	-	-	10
Ag/HfO_2/CDs/Pt	0.18	-0.08	10^4	2.4×10^5	This work

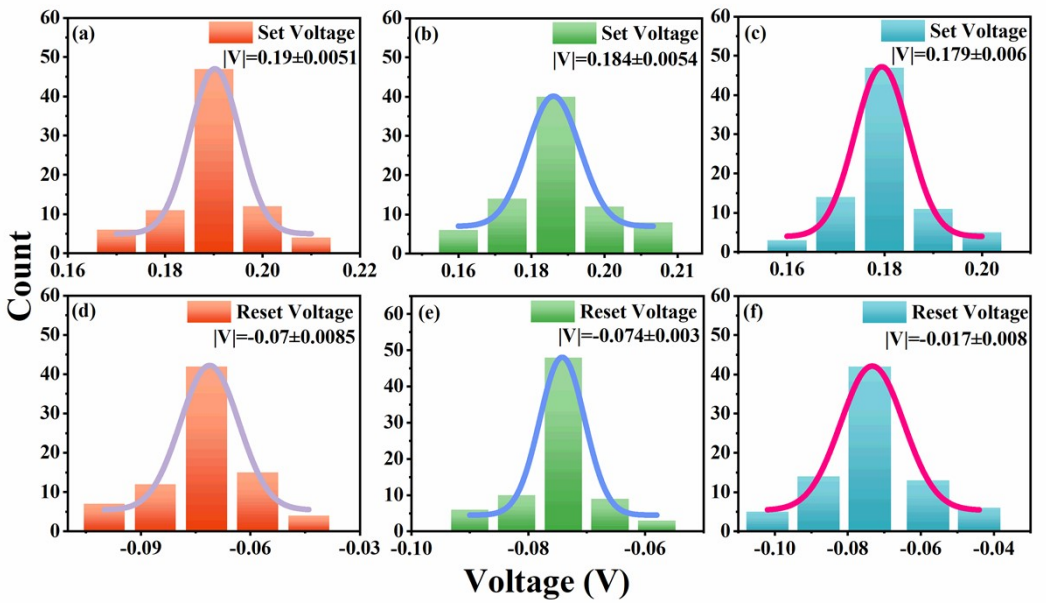

Fig. S3 SET voltages distribution of the first (a), second (b), and third (c) batches of CDMDs. RESET voltages distribution of the first (d), second (e), and third (f) batches of CDMDs. The curves are Gaussian fits to the histograms.

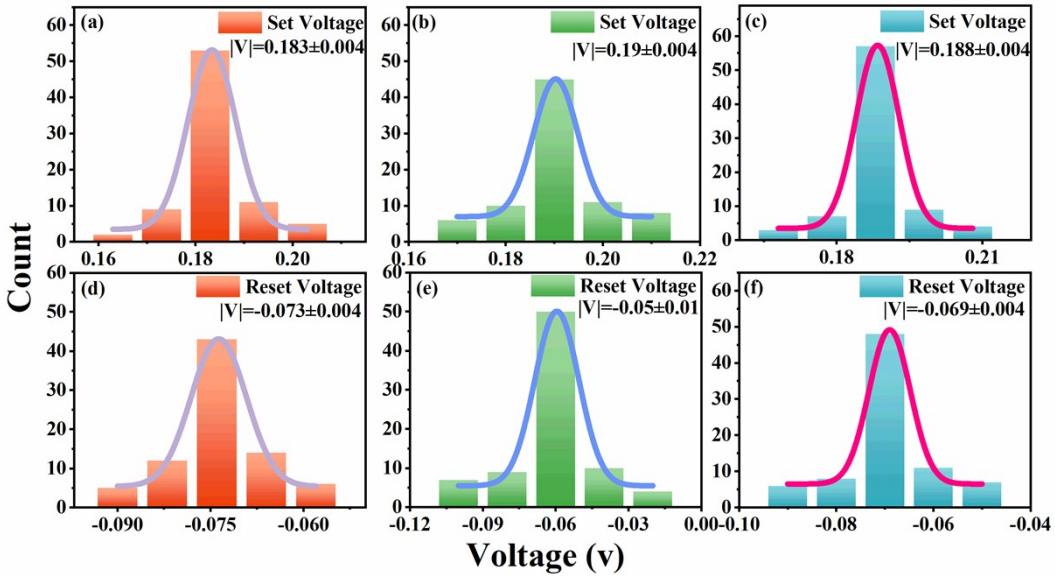

Fig. S4 SET voltages distribution of the first (a), second (b), and third (c) devices of CDMDs. RESET voltages distribution of the first (d), second (e), and third (f) devices of CDMDs. And the curves are Gaussian fits to the histograms.

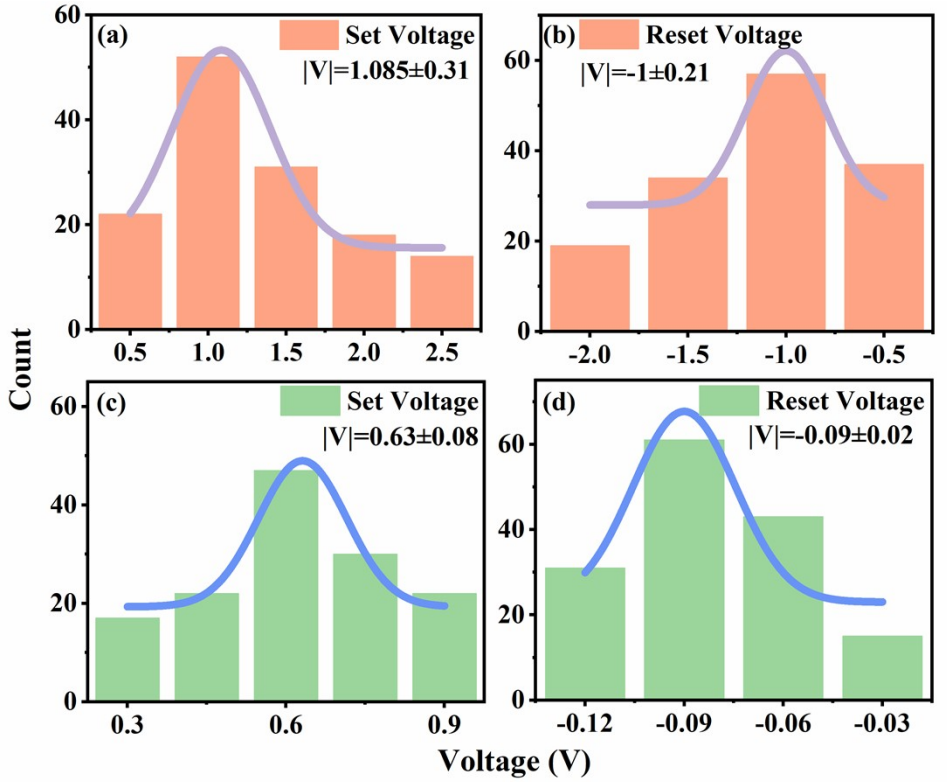

Fig. S5 SET voltages and RESET voltages distribution of Ag/MoO_3/Pt (a, b) and Ag/ZrO_2/Pt (c, d) memristors, respectively. And the curves are Gaussian fits to the histograms.

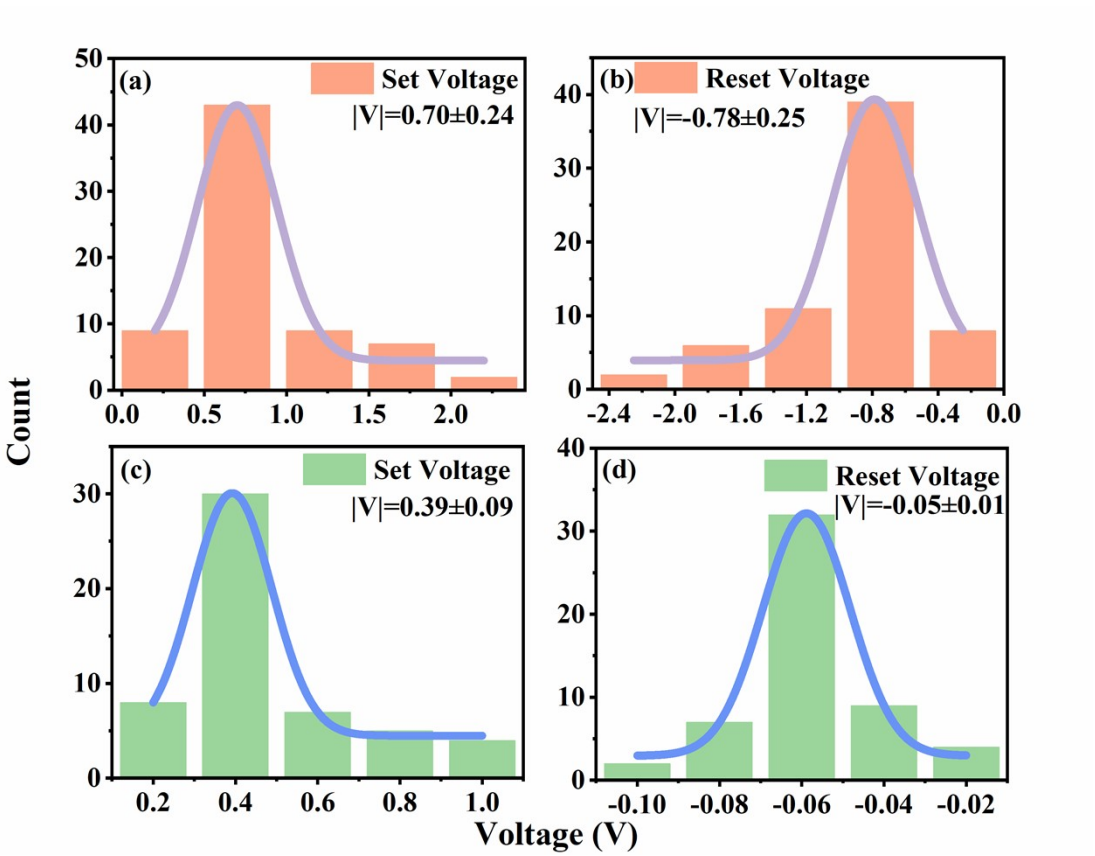

Fig. S6 SET voltages and RESET voltages distribution of Ag/MoO_3/CDs/Pt (a, b) and Ag/ZrO_2/CDs/Pt (c, d)

memristors, respectively. And the curves are Gaussian fits to the histograms.

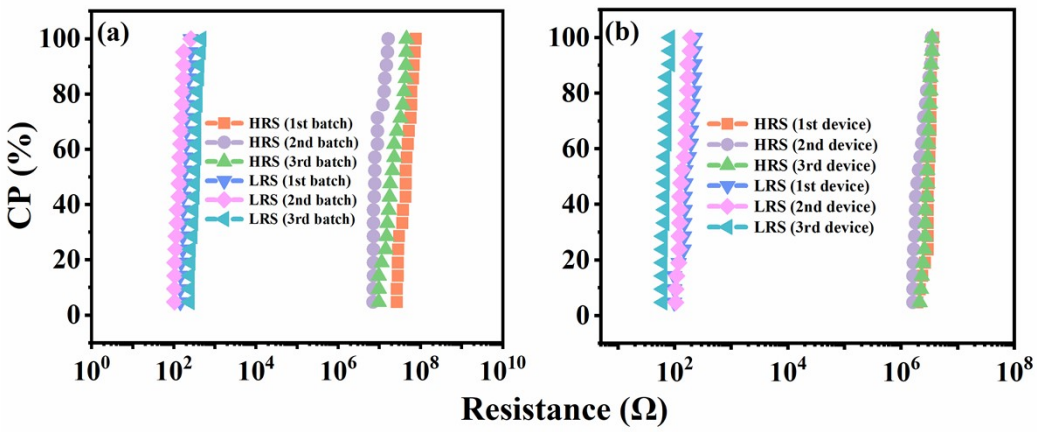

Fig. S7 Resistance distribution Statistics of three batches (a) and three devices (b) of CDMDs.

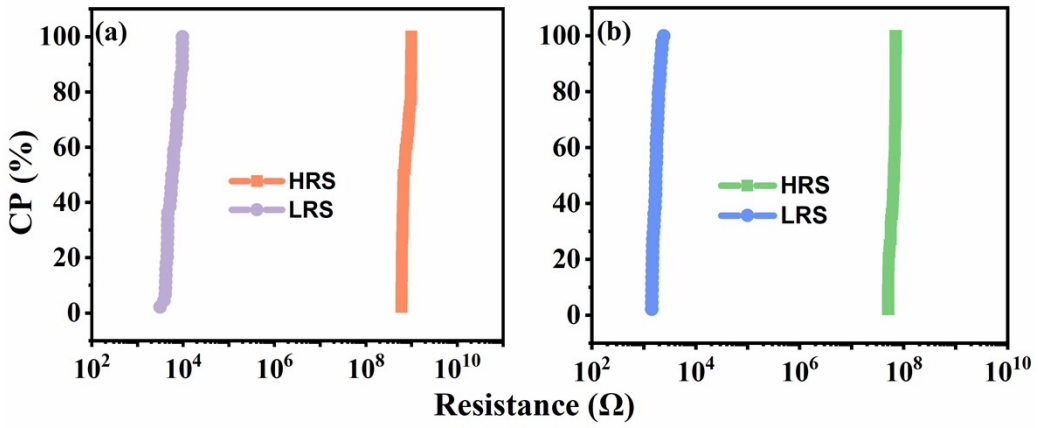

Fig. S8 Resistance distribution statistics of (a) CDMDs (MoO_3), (b) CDMDs (ZrO_2).

I STDP learning function

$$\xi = \begin{cases} A_+ \exp(-\dfrac{\Delta t_{post-pre}}{\tau_+}) & (\Delta t_{post-pre} > 0) \\ -A_- \exp(-\dfrac{\Delta t_{post-pre}}{\tau_-}) & (\Delta t_{post-pre} < 0) \end{cases} \quad \text{(S1)}$$

where A_+ and A_- were defined as the maximum synaptic strength modification when $\Delta t_{post-pre}$ is near zero. τ_+ and τ_- are learning windows determining.

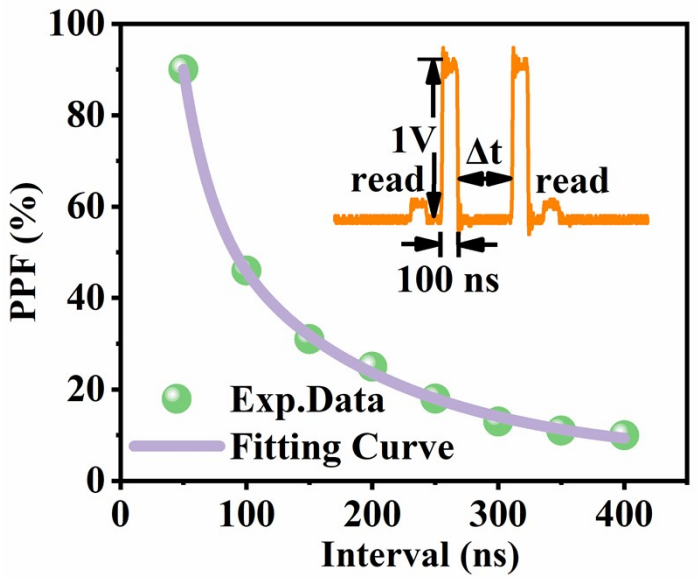

Fig. S9 Paired-pulse facilitation (PPF) characteristics of CDMDs and the waveform used for PPF measurement. The purple line shows the empirical fitting result obtained by using Equation (S2).

II Simulates the PPF functions of biological synapses

The PPF ratio is defined by

$$PPF = \frac{G_2 - G_1}{G_1} \times 100\% = C_1 \times e^{\frac{-t}{\tau_1}} + C_2 \times e^{\frac{-t}{\tau_2}} \quad \text{(S2)}$$

Here, G_1 and G_2 are the conductance values after the first and second pulses, respectively. The two fitting time constants τ_1 (21 ns) and τ_2 (142 ns) are relevant to fast and slow decaying terms, respectively.

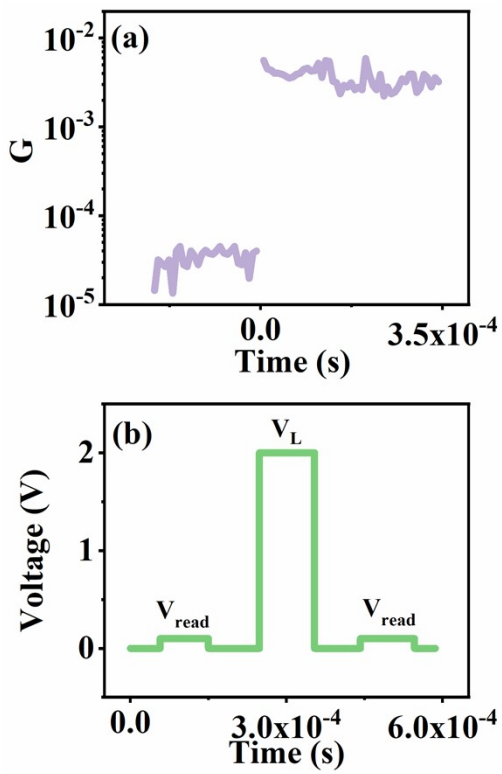

Fig. S10 Only formal learning process waveform (b) and conductance state (a).

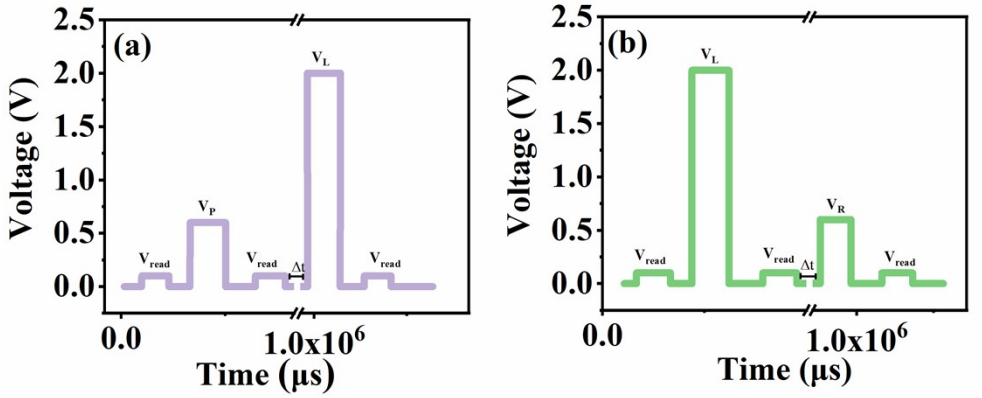

Fig. S11 Waveforms applied to the device, representing the preview (a) and review (b) processes respectively.

References

1. S. Liu, N. Lu, X. Zhao, H. Xu, W. Banerjee, H. Lv, S. Long, Q. Li, Q. Liu and M. Liu, Eliminating negative-SET behavior by suppressing nanofilament overgrowth in cation-based memory, *Advanced Materials*, 2016, **28**, 10623-10629.

2. N. Ilyas, D. Li, C. Li, X. Jiang, Y. Jiang and W. Li, Analog switching and artificial synaptic behavior of Ag/SiO x: Ag/TiO x/p++-Si memristor device, *Nanoscale research letters*, 2020, **15**, 1-11.

3. Y. Zhang, Y. Li, X. Wang and E. G. Friedman, Synaptic characteristics of Ag/AgInSbTe/Ta-

based memristor for pattern recognition applications, *IEEE Transactions on Electron Devices*, 2017, **64**, 1806-1811.

4. X. Yan, C. Qin, C. Lu, J. Zhao, R. Zhao, D. Ren, Z. Zhou, H. Wang, J. Wang and L. Zhang, Robust Ag/ZrO2/WS2/Pt memristor for neuromorphic computing, *ACS applied materials & interfaces*, 2019, **11**, 48029-48038.

5. B. G. Chae, J. B. Seol, J. H. Song, K. Baek, S. H. Oh, H. Hwang and C. G. Park, Nanometer-Scale Phase Transformation Determines Threshold and Memory Switching Mechanism, *Advanced materials*, 2017, **29**, 1701752.

6. A. Moudgil, N. Kalyani, G. Sinsinbar, S. Das and P. Mishra, S-layer protein for resistive switching and flexible nonvolatile memory device, *ACS applied materials & interfaces*, 2018, **10**, 4866-4873.

7. W. Li, J. Liu, Y. Yu, G. Feng, Y. Song, Q. Liang, L. Liu, S. Lei and W. Hu, Synthesis of large-area ultrathin graphdiyne films at an air–water interface and their application in memristors, *Materials Chemistry Frontiers*, 2020, **4**, 1268-1273.

8. L. Zhou, J. Y. Mao, Y. Ren, J. Q. Yang, S. R. Zhang, Y. Zhou, Q. Liao, Y. J. Zeng, H. Shan and Z. Xu, Biological spiking synapse constructed from solution processed bimetal core–shell nanoparticle based composites, *Small*, 2018, **14**, 1800288.

9. T. Dongale, S. Shinde, R. Kamat and K. Rajpure, Nanostructured TiO2 thin film memristor using hydrothermal process, *Journal of Alloys and Compounds*, 2014, **593**, 267-270.

10. J. Wang, Z. Lv, X. Xing, X. Li, Y. Wang, M. Chen, G. Pang, F. Qian, Y. Zhou and S. T. Han, Optically modulated threshold switching in core–shell quantum dot based memristive device, *Advanced Functional Materials*, 2020, **30**, 1909114.

11. M. Kim, S. Oh, S. Song, J. Kim and Y.-H. Kim, Solution-Processed Memristor Devices Using a Colloidal Quantum Dot-Polymer Composite, *Applied Sciences*, 2021, **11**, 5020.

12. Z. Zhou, H. Mao, X. Wang, T. Sun, Q. Chang, Y. Chen, F. Xiu, Z. Liu, J. Liu and W. Huang, Transient and flexible polymer memristors utilizing full-solution processed polymer nanocomposites, *Nanoscale*, 2018, **10**, 14824-14829.

13. S. K. Ganeshan, V. Selamneni and P. Sahatiya, Water dissolvable MoS 2 quantum dots/PVA film as an active material for destructible memristors, *New Journal of Chemistry*, 2020, **44**, 11941-11948.

14. A. Thomas, A. Resmi, A. Ganguly and K. Jinesh, Programmable electronic synapse and nonvolatile resistive switches using MoS 2 quantum dots, *Scientific reports*, 2020, **10**, 1-10.

15. K. Chang, X. Yu, B. Liu, Y. Niu, R. Wang, P. Bao, G. Hu and H. Wang, Quantum-Dots Optimized Electrode for High-Stability Transient Memristor, *IEEE Electron Device Letters*, 2021, **42**, 824-827.

16. S. Ali, J. Bae, C. H. Lee, K. H. Choi and Y. H. Doh, All-printed and highly stable organic resistive switching device based on graphene quantum dots and polyvinylpyrrolidone composite, *Organic Electronics*, 2015, **25**, 225-231.

17. S. K. Meladom, S. Arackal, A. Sreedharan, S. Sagar and B. C. Das, Microwave assisted robust aqueous synthesis of Mn 2+-doped CdSe QDs with enhanced electronic properties, *Rsc Advances*, 2018, **8**, 26771-26781.

18. M. Dragoman, A. Dinescu, D. Dragoman, C. Palade, A. Moldovan, M. Dinescu, V. Teodorescu and M. Ciurea, Wafer-scale graphene-ferroelectric HfO2/Ge–HfO2/HfO2 transistors acting as three-terminal memristors, *Nanotechnology*, 2020, **31**, 495207.

19. A. S. Sokolov, M. Ali, R. Riaz, Y. Abbas, M. J. Ko and C. Choi, Silver-adapted diffusive memristor based on organic nitrogen-doped graphene oxide quantum dots (N-GOQDs) for artificial biosynapse applications, *Advanced Functional Materials*, 2019, **29**, 1807504.